

ONCOGENOMICS

Genomic profiling of malignant melanoma using tiling-resolution arrayCGHG Jönsson¹, C Dahl², J Staaf¹, T Sandberg¹, P-O Bendahl¹, M Ringnér³, P Guldberg² and Å Borg¹¹Department of Oncology, University Hospital, Lund, Sweden; ²Institute of Cancer Biology, Danish Cancer Society, Strandboulevarden, Copenhagen, Denmark and ³Department of Theoretical Physics, Lund University, Lund, Sweden

Malignant melanoma is an aggressive, heterogeneous disease where new biomarkers for diagnosis and clinical outcome are needed. We searched for chromosomal aberrations that characterize its pathogenesis using 47 different melanoma cell lines and tiling-resolution bacterial artificial chromosome-arrays for comparative genomic hybridization. Major melanoma genes, including *BRAF*, *NRAS*, *CDKN2A*, *TP53*, *CTNNB1*, *CDK4* and *PTEN*, were examined for mutations. Distinct copy number alterations were detected, including loss or gain of whole chromosomes but also minute amplifications and homozygous deletions. Most common overlapping regions with losses were mapped to 9p24.3–q13, 10 and 11q14.1–qter, whereas copy number gains were most frequent on chromosomes 1q, 7, 17q and 20q. Amplifications were delineated to oncogenes such as *MITF* (3p14), *CCND1* (11q13), *MDM2* (12q15), *CCNE1* (19q12) and *NOTCH2* (1p12). Frequent findings of homozygous deletions on 9p21 and 10q23 confirmed the importance of *CDKN2A* and *PTEN*. Pair-wise comparisons revealed distinct sets of alterations, for example, mutually exclusive mutations in *BRAF* and *NRAS*, mutual mutations in *BRAF* and *PTEN*, concomitant chromosome 7 gain and 10 loss and concomitant chromosome 15q22.2–q26.3 gain and 20 gain. Moreover, alterations of the various melanoma genes were associated with distinct chromosomal imbalances suggestive of specific genomic programs in melanoma development.

Oncogene (2007) 26, 4738–4748; doi:10.1038/sj.onc.1210252; published online 29 January 2007

Keywords: melanoma; arrayCGH; mutation

Introduction

Cutaneous malignant melanoma (CMM) is an aggressive form of skin cancer with increasing incidence in the Western world (Tucker and Goldstein, 2003). CMM has

a heterogeneous and unpredictable clinical course with a potential for aggressive growth and refractoriness to available chemotherapy. The risk of CMM is influenced by both genetic and environmental factors, and the incidence varies between populations depending on pigmentation, skin type and sun exposure. An established risk factor for CMM is a family history of the disease. Two high-penetrance susceptibility genes, *CDKN2A* (primarily the p16INK4A sequence) and *CDK4*, have been identified, but germ-line mutations in these genes account for merely one-third of high-risk families, implicating the existence of additional melanoma genes (Hayward, 2003).

Several studies have addressed the genetic events in sporadic CMM development. Somatic inactivation of *CDKN2A* (p16INK4A and p14ARF) is frequently detected in melanoma cell lines but less commonly in primary tumors (Cachia *et al.*, 2000). More recent reports show biallelic *CDKN2A* deletions in ~45% of CMM metastases emphasizing this locus in disease progression (Grafstrom *et al.*, 2005). Activation of the mitogen-activated protein kinase (MAPK) pathway may also be a compulsory event in CMM pathogenesis, primarily evident as either *BRAF* (60% of melanomas) or *NRAS* (30%) point mutations, but never both (Maldonado *et al.*, 2003; Omholt *et al.*, 2003). Known to be early events and present in benign nevi (Pollock *et al.*, 2003), *BRAF* mutations may influence tumor progression and give rise to distinct gene expression signatures in melanoma cell lines (Pavey *et al.*, 2004). Gain of chromosome 7q is common in CMM suggesting that *BRAF*, located on 7q34, is a target for gene amplification (Tanami *et al.*, 2004). Moreover, cyclin D1, a down-stream target of the MAPK pathway and p16INK4A antagonist, is amplified in acral-type CMM in which *BRAF* and *NRAS* mutations are infrequent (Takata *et al.*, 2005). Finally, activation of the PIK3-pathway is essential and commonly pursued by inactivation of *PTEN* located on chromosome 10, a frequent deletion target in melanoma (Guldberg *et al.*, 1997b).

A recent genome-wide survey in melanocytic lesions, using array-based comparative genomic hybridization (arrayCGH), revealed patterns of genomic aberrations that could distinguish chronically sun-induced from non-sun-induced melanomas and further classify tumors into clinically relevant groups (Curtin *et al.*, 2005). Here, we used CGH to arrays of 32433 bacterial artificial

Correspondence: Professor Å Borg, Department of Oncology, Lund University, Lund SE-221 85, Sweden.

E-mail: ake.borg@med.lu.se

Received 7 August 2006; revised 2 November 2006; accepted 23 November 2006; published online 29 January 2007

chromosome (BAC) clones forming a contiguous and tiling coverage of the human genome with an average resolution of ~100 kbp, to precisely map novel DNA copy number gains and losses in 47 melanoma cell lines thoroughly characterized also for mutations in the known major melanoma genes. In addition, the study reveals that mutants *BRAF*, *NRAS*, *PTEN* or *TP53* are associated with discrete chromosomal alterations, possibly reflecting cooperative events in melanoma pathogenesis.

Results

DNA copy number profiles were established in cell lines originating from 46 different metastatic CMM and one primary ocular melanoma (Figure 1). The overall genome patterns are complex, involving whole chromosome gains and losses as well as focal alterations such as narrow amplifications and homozygous deletions (Figure 2). Only one (EST97) of the 47 cell lines had no apparent alterations using the current technology. Combining data from all cell lines, alterations were found on all chromosomes at least once. Chromosomal arms with copy number gains in at least 50% of the cell lines included 1q, 7p, 7q, 8q, 17q and 20q. Frequent

losses were found on 4p, 4q, 6q, 8p, 9p, 10p, 10q and 11q (Figure 2a).

Regions showing frequent copy number losses and gains

The two most common individual copy number losses were detected on chromosomes 10 and 9p24.3–q13, both spanning over large genomic regions harboring known melanoma tumor suppressor genes, that is, *PTEN* and *CDKN2A*, which were further pinpointed in some cell lines by homozygous deletions (see below). Other regions frequently affected by large genomic deletions localize to chromosomes 4, 6q and 11q. The smallest regions of overlapping (SRO) losses span 6q23.3–q25.3 and 11q22.3–q24.1, including a large number of candidate genes, whereas complete loss was the most common chromosome 4 aberrations. Restricted deletions were also present on chromosome 1p in ~50% of the samples, and the SRO loss was further narrowed down to two loci. The first maps to 1p22.1 (92029228–94254061 bp; UCSC May 2004 build hg17) and includes ~20 genes, for instance *TGFBR3* and *CDC18*. The second region maps to 1p21.3 (95472183–98455030 bp) and includes only two known coding genes, *PTBP2* and *DPYD*, and a putative microRNA, *miR-137*. Moreover, chromosome 9q was deleted in ~40% of the cell lines with an SRO on 9q21.13–q21.2 (72394581–78138360 bp).

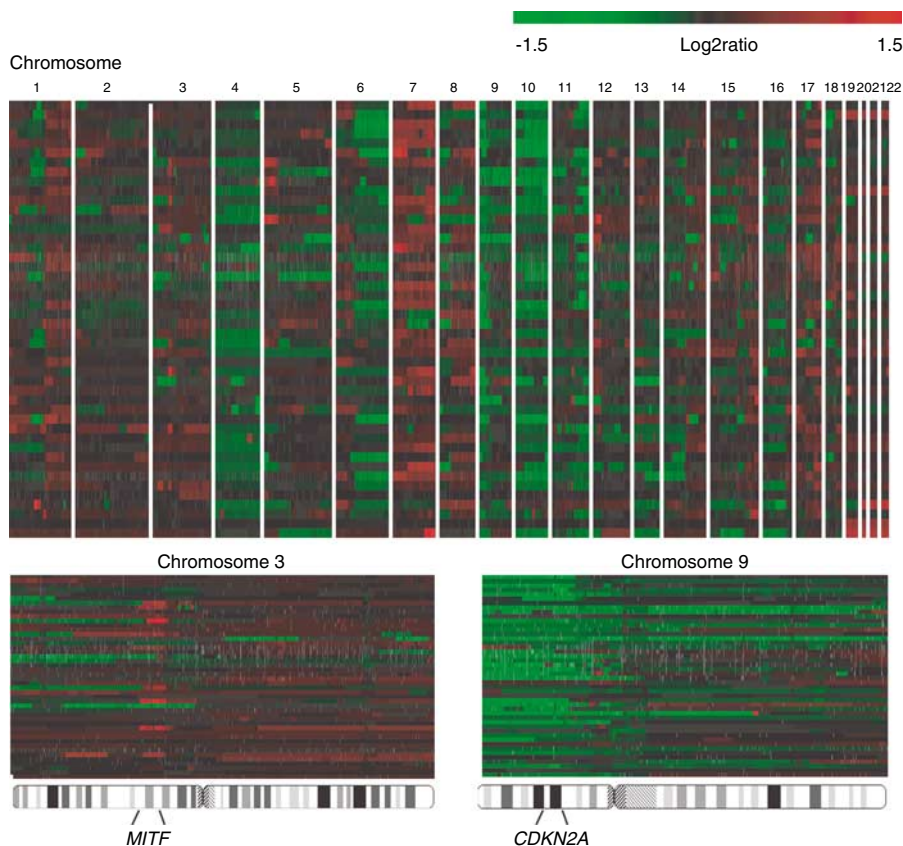


Figure 1 Heat-map over DNA copy number aberrations (x-axis) in 47 melanoma cell lines (y-axis). Red represents gains/amplifications and green represents loss/homozygous deletions. Bottom left panel zoom-in on chromosome 3, depicting the frequent DNA copy number gains at the *MITF* locus at 3p13. Bottom right panel displays chromosome 9 and the common DNA copy number losses on the p-arm, occasionally limited to 9p21.3 and *CDKN2A* homozygous deletions.

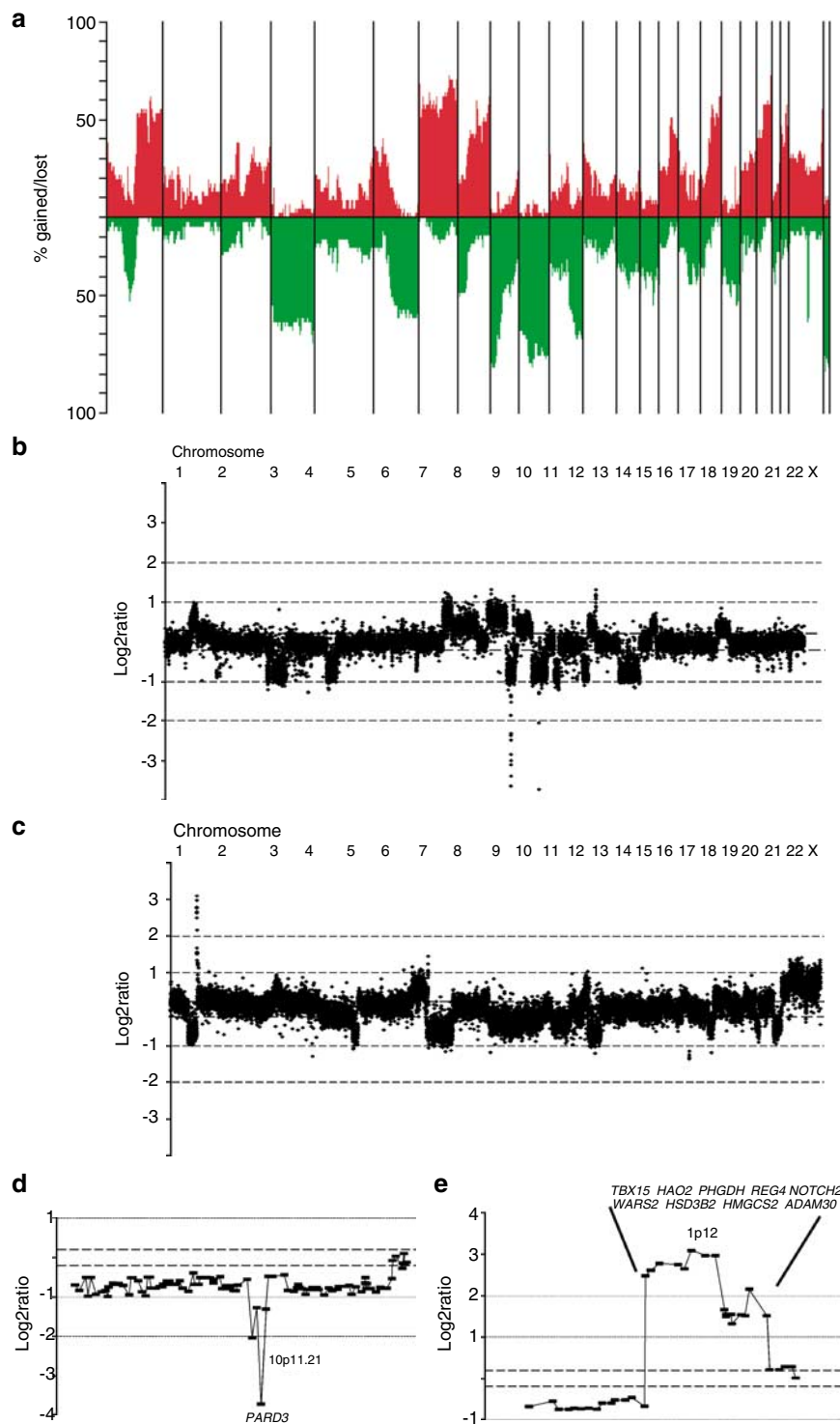


Figure 2 (a) Genome-wide frequency plot of DNA copy number gains (red) and losses (green) for all 47 melanoma cell lines. (b) Genomic profile of EST73 cells. Homozygous deletions are clearly seen at chromosome 9p21.3 (*CDKN2A*) and 10p11.21 (*PARD3*). (c) Genomic profile of FM79 cells. Distinct amplification at chromosome 1p12 (*NOTCH2* and other genes). (d) Zoom-in on chromosome 10p11 displaying a homozygous deletion of the *PARD3* gene in EST73 cells. (e) Zoom-in on chromosome 1p12 displaying one the recurrently amplified regions including the *NOTCH2* gene.

Chromosomal regions displaying frequent DNA copy number gains include 1q, 7, 8q, 17q and 20q. The SRO gain on 1q23.3–q25.3 (157822335–181823355 bp) spans ~24 Mbp and contains a large number of genes. The

SRO gains on chromosome 7 were divided into two distinct loci. The first (found in 59%) maps to 7q21.13–q31.1 (87891721–107605147 bp) and includes *CDK6*, whereas the second (65%) is more distal (7q32.1–q34;

126600073–142561955 bp) and includes *BRAF*. Furthermore, two SRO gains were detected on chromosome 8, the first maps to 8q22.1–q22.3 (96297981–104661726 bp) and the second to 8q24.11–q24.22 (118528414–134896260 bp) and includes *MYC*. Copy number gains on chromosome 17 were observed in ~50% of the cell lines and two SRO gains map to 17q23.2–q24.1 (55386720–60690169 bp) and 17q25.1–q25.3 (69684458–74597283 bp), respectively. Finally, two SRO gains on chromosome 20 map to 20q12–q13.12 (38554072–45485732 bp) and 20q13.31–q13.33 (54727799–62434349 bp), respectively.

High-level amplifications

More narrow peaks corresponding to focal amplifications (defined as \log_2 ratio > 1.5) were detected at 25 loci in 15 different cell lines (Table 1). Recurrent amplifications were located on 11q13, 3p14 and 1p12. The 11q13 amplicon includes *CCND1* and was seen in three cell lines. Chromosome 3p14, including the melanoma oncogene microphthalmia-associated transcription factor (*MITF*), was amplified in three cell lines and *MITF* copy number gain was found in additional cell lines, in total 36%. Chromosome 1p12 was amplified in three cell lines, one (FM79) of which harbored a narrow peak including only *NOTCH2*. Other known amplified oncogenes include *CCNE1* on 19q13, *MDM2* on 12q15 and *BRAF* on 7q34. Moreover, 13 additional amplicons without obvious target genes were identified (Table 1).

Homozygous deletions

Previously recognized homozygous deletions on chromosomes 9p21.3 and 10q23.31 were confirmed and shown to target *CDKN2A* and *PTEN*, respectively, often as the single-affected gene (Table 1). Moreover, two novel homozygous deletions including single genes, 10p11.22 (*PARD3*) and 11q14.1 (*RAB38*), were detected. A recurrent homozygous deletion on 4q34.3 including no known genes was found in three cell lines.

Mutation screening

BRAF, *NRAS*, *PTEN*, *TP53*, *CDKN2A*, *CDK4* and *CTNNB1* were analysed for mutations. Two-thirds ($n = 32$) of the 47 cell lines contained a *BRAF* mutation, in all but one the V600E mutation. Ten (21%) cell lines had *NRAS* mutation, all at codon 61. Six cell lines harbored neither *BRAF* nor *NRAS* mutations, including the ocular melanoma EST128 and EST97, the latter devoid of CGH alterations. *TP53* mutations were present in 31%, whereas *PTEN* mutations were identified in 27% of the cell lines. *CDKN2A* was inactivated by point mutations, homozygous deletions or methylation in 10, 57 and 10%, respectively, any form of inactivation being found in 77% of the cell lines. In addition, one cell line (FM56) harbored a mutation in *CDK4* and another (FM9) contained a *CTNNB1* mutation (Table 1). Accordingly, the mutation frequency (below in parentheses) seen here in 47 melanoma cell lines is similar to the Cancer Genome Project

database (<http://www.sanger.ac.uk/genetics/CGP/>) on 46 (other) malignant melanoma cell lines: *BRAF* 60% (63%), *CDKN2A* 54% (77%), *TP53* 32% (31%), *NRAS* 21% (21%) and *PTEN* 17% (27%).

Correlation of cancer gene mutation status and genetic alterations

Two-sided *t*-test was performed to determine whether *PTEN*, *TP53*, *BRAF* or *NRAS* mutation status was associated with specific DNA copy number aberrations. Indeed, mutation in *PTEN* was correlated ($P < 0.05$) to loss of 1p22.1–p21.1, a region spanning ~10 Mbp and >50 known genes. Other altered regions overrepresented in *PTEN*-mutated cell lines included 10q loss, 13q14–q33 loss, 14q21–q23 loss and 19q13 gain ($P < 0.05$). Mutation in *TP53* was inversely correlated ($P < 0.05$) to 1p34.3–p13.2 loss, in fact, *TP53*-mutated cell lines were instead associated with gains at 1p34.3–p13.2. Moreover, 5q35 gain, 12q14 loss and 12q15–q21 loss distinguished *TP53* mutated from wild-type cells ($P < 0.05$) (Figure 4). Cells with *BRAF* mutation had a higher frequency of chromosome 7 gains, often comprising large regions and always including *BRAF* on 7q34 ($P < 0.05$). Chromosome 7 gains were also seen in cell lines with wild-type *BRAF* and *NRAS*; however, less commonly in *NRAS*-mutated cells. Also, 2p11–q13 gain, 6p22 loss, 10 loss, 11q loss, 14q21–q23 loss and 20 gain were more frequently observed in *BRAF* mutant cell lines ($P < 0.05$). Alterations specific for *NRAS*-mutated cells included only 3q13.12–q13.31 gain ($P < 0.05$), although regions commonly altered in *BRAF*-mutated and wild-type cells (chromosome 7 and 20) were less frequently affected in *NRAS*-mutant cells (Figure 3). Furthermore, *BRAF* and *NRAS* mutations were found to be mutually exclusive ($P < 0.00001$), *PTEN* and *NRAS* mutations were rarely mutual ($P = 0.038$), whereas combined *BRAF* and *PTEN* mutations were common ($P = 0.0023$). No correlation was found between *TP53* mutations and mutations in other genes.

Concomitant copy number alterations

Regions that are affected by DNA copy number changes in at least 40% of the cell lines, including eight gains and eight losses (as defined in Materials and methods), were analysed to detect patterns in copy number aberrations. Twelve pairs of aberrations were seen significantly more often than expected under the null hypothesis of independent genetic events ($P < 0.05$) (Table 2). The highest correlation between alterations not affecting the same chromosomal arm was seen for 8p23.3–p23.1 loss and 8q12.1–q23.1 gain. Significant correlation was also seen for gain of chromosome 7 (where *BRAF* resides) and loss of chromosome 10 (*PTEN*).

Discussion

CMM is an aggressive, heterogeneous disease where new markers for diagnosis, prognosis and treatment effect are needed. Genomic and gene expression profiling are

**Table 1** Gene alterations in cell lines derived from 46 CMM and one ocular melanoma (EST128)

Cell line	<i>BRAF</i> mutation	<i>NRAS</i> mutation	<i>CDKN2A</i> status	<i>PTEN</i> status	<i>TP53</i> mutation	Focal amplification	Gene-specific HD
EST128	—	—	—	—	—	—	—
EST133	V600E	—	c.238 C>T	—	—	—	—
EST135	V600E	—	methylation	—	ca. 527 G>A	8q24.13, 8q21.13, 22q13.1	—
EST45	—	Q61R	HD (exon 1–3)	—	—	1p12–p13.1, 10q22.1, 19p12–p13.11	<i>CDKN2A</i>
EST50	—	—	c.237_238 delinsTT	—	c. 949 C>T	<i>CCND1</i> , 9q22.33–q31.1	—
EST57	V600E	—	HD (exon1–3)	—	—	—	<i>CDKN2A</i>
EST69	—	Q61R	HD (exon 1–3)	—	—	<i>MDM2</i> , 18q11.2	<i>CDKN2A</i>
EST70	—	Q61L	c.143 C>T	—	c. 853 G>A	—	—
EST71	V600E	—	c.225_243 dup19	HD (exon 4–9)	—	—	<i>PTEN</i>
EST73	V600E	—	HD (exon 1–3)	c. 634 + 5G>T	c. 743 G>A	—	<i>CDKN2A PARD3</i>
EST74	—	—	HD (exon 1–3)	—	—	—	<i>CDKN2A^a</i>
EST75	V600E	—	HD (exon 1–3)	—	—	<i>CCND1</i> , 1p12–p11.2	<i>CDKN2A</i>
EST79	—	—	—	—	c. 724 T>G	1p22.2–p21.3	—
EST81	V600E	—	—	—	c. 659 A>G	<i>MITF</i> , <i>CCND1</i>	—
EST84	—	Q61R	HD (exon1–3)	—	c. 722 C>T	—	<i>CDKN2A</i>
EST94	—	Q61K	HD (exon 1–3)	—	—	—	<i>CDKN2A</i>
EST97	—	—	—	—	—	—	—
FM116	V600E	—	HD (exon 1–3)	—	—	—	<i>CDKN2A</i>
FM2	—	Q61R	—	HD (exon 6)	—	—	<i>PTEN</i>
FM28	—	Q61K	HD (exon 2–3)	—	—	3p12.1–p11.1	<i>CDKN2A^a</i>
FM3	—	—	HD (exon 1–3)	—	—	—	<i>CDKN2A^a</i>
FM45	V600E	—	HD (exon 1–3)	—	—	—	<i>CDKN2A</i>
FM48	V600E	—	HD (exon 1–3)	—	—	—	<i>CDKN2A</i>
FM55II	V600E	—	—	—	c. 949 C>T	4q28.3–q32.1	—
FM56	V600E	—	—	—	—	<i>CCNE1</i>	—
FM57	V600K	—	HD (exon 1–3)	—	—	—	<i>CDKN2A^a</i>
FM58	V600E	—	HD (exon 1–3)	—	—	—	<i>CDKN2A</i>
FM6	—	Q61K	Methylation	—	—	—	—
FM62	V600E	—	HD (exon 1)	L139X	—	—	<i>CDKN2A^a</i>
FM66	V600E	—	HD (exon 1–3)	—	—	—	<i>CDKN2A</i>
FM69	V600E	—	HD (exon 1–3)	—	—	—	<i>CDKN2A^a</i>
FM72	V600E	—	HD (exon 1–3)	HD (exon 2–3)	—	5p	<i>CDKN2A PTEN</i>
FM74	—	Q61L	—	—	—	—	—
FM76	V600E	—	HD (exon 1–3)	—	—	—	<i>CDKN2A^a</i>
FM78	V600E	—	HD (exon 1–3)	—	c. 815 T>G	—	<i>CDKN2A^a</i>
FM79	—	Q61L	Methylation	—	—	1p12–p11.2	—
FM82	V600E	—	HD (exon 2–3)	HD (exon 4–9)	—	—	<i>CDKN2A^a PTEN</i>
FM86	—	—	c.171_172 delinsTT	—	—	—	—
FM88	V600K	—	HD (exon 1–3)	c. 380 G>A	—	—	<i>CDKN2A^a</i>
FM9	V600E	—	HD (exon 1–3)	c. 640 C>T	—	—	<i>CDKN2A</i>
FM92	V600E	—	—	HD (exon 2–9)	—	—	<i>RAB38 PTEN</i>
FM93	V600E	—	HD (exon 1–3)	—	c.795–796 GG>AA	<i>MITF</i>	<i>CDKN2A^a</i>
FM95	L596S	—	Methylation	HD (exon 1–2)	c. 541 C>T	<i>BRAF</i>	<i>PTEN</i>
SK-MEL-19	V600E	—	HD (exon 1–3)	—	—	—	<i>CDKN2A^a</i>
SK-MEL-28	V600E	—	—	T167A A>G	L145R T>G	<i>MITF</i> , 20q13.33, 20q11.23	—
SK-MEL-3	V600E	—	Methylation	—	R267W C>T	—	—
SK-MEL-31	V600E	—	HD (exon 1–3)	HD (exon 6–9)	—	—	<i>CDKN2A^a PTEN^a</i>

Mutations are defined as amino acid substitutions (*BRAF* and *NRAS*), or coding nucleotide change, HD or methylation (*CDKN2A*, *PTEN*, *TP53*). Focal amplification was defined as log 2 ratio > 1.5 and listed as defined target gene or chromosomal region. ^aHomozygous deletion not detectable by array CGH. CMM, cutaneous malignant melanoma; HD, homozygous deletion.

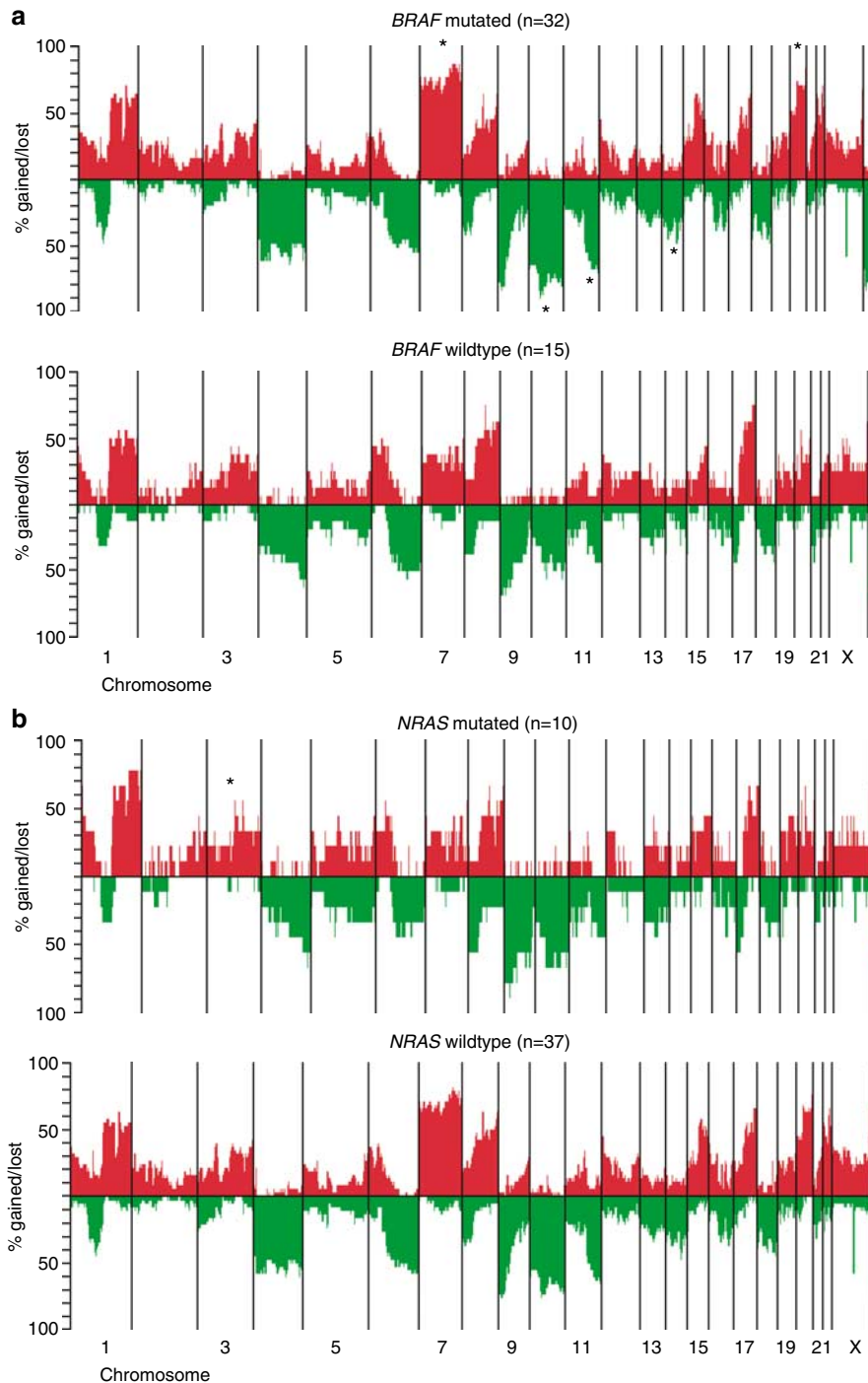


Figure 3 (a) DNA copy number frequency plots for *BRAF*-mutated (upper panel) and wild-type cell lines (lower panel). Regions altered significantly ($P < 0.05$) more frequent in *BRAF* mutant compared to wild-type cell lines are indicated (*) in the upper panel. (b) DNA copy number frequency plots for *NRAS*-mutated (upper panel) and wild-type cell lines (lower panel). The region (3q13.12–q13.31) altered (gained) significantly ($P < 0.05$) more frequent in *NRAS* mutant compared to wild-type cell lines is indicated (*) in the upper panel.

powerful tools in this respect, for example, revealing gene sets that allow discrimination of vertical and radial growing CMM and that can be used for class discovery (Bittner *et al.*, 2000; Haqq *et al.*, 2005). Moreover, arrayCGH unraveled genomic aberrations specific for chronic sun-induced melanomas, and indicated that

alteration in the CDKN2A and PI3K pathways are independent but complementary events in melanoma pathogenesis (Curtin *et al.*, 2005).

Here, in a screen of 47 melanoma cell lines using tiling BAC-arrayCGH, we confirm the high frequency of chromosome 9p24.3–q13 and 10 loss, encompassing

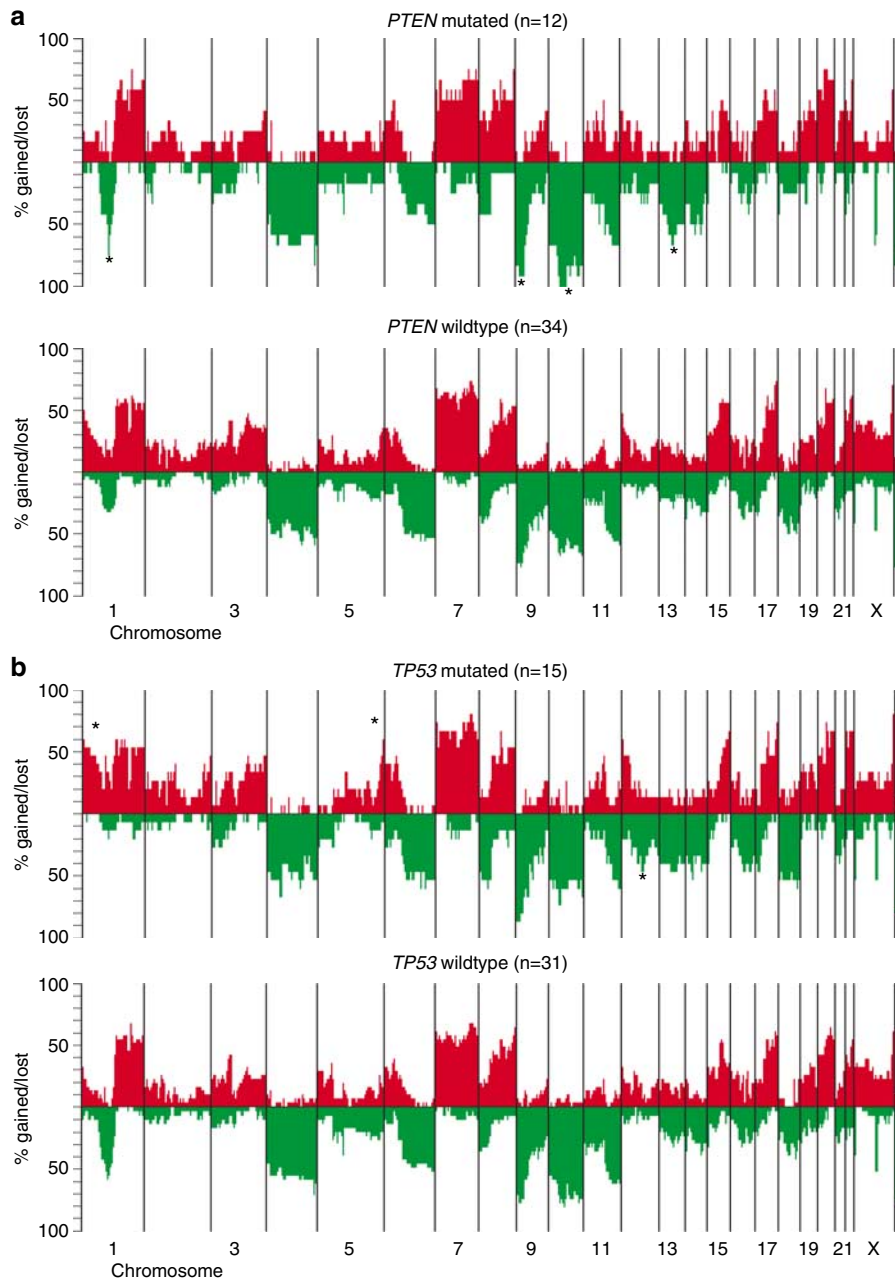


Figure 4 (a) DNA copy number frequency plots for *PTEN*-mutated (upper panel) and wild-type cell lines (lower panel). Regions altered significantly ($P < 0.05$) more frequent in *PTEN* mutant compared to wild-type cell lines are indicated (*) in the upper panel. Chromosomes 1p, 9p, 10 and 13q losses are significantly more common in *PTEN* mutated cell lines. (b) DNA copy number frequency plots for *TP53* mutated (upper panel) and wild-type cell lines (lower panel). Regions altered significantly ($P < 0.05$) more frequent in *TP53* mutant compared to wild-type cell lines are indicated (*) in the upper panel. Chromosome 1p and 5q35 gains and losses at 12q14 and 12q15–q21 are significantly more common in *TP53*-mutated cell lines.

CDKN2A (9p21.3) and *PTEN* (10q23.31). Of interest is the novel melanoma susceptibility locus on 1p identified by linkage analysis and mapped by critical recombinants in linked families to a 15 Mbp region between D1S430 and D1S2664 at 1p31.1–1p21.3 (Gillanders *et al.*, 2003). It was shown that 80% of familial tumors exhibited loss of heterozygosity at this region, with an SRO deletions of 9 Mbp between D1S207 and D1S435 at 1p31.1–1p22.2 (Walker *et al.*, 2004), strongly suggestive

of a classical tumor suppressor gene locus. Our data indicate two SRO losses in this region. The first maps to 1p22.1 and includes candidate genes such as *TGFBR3* and *CDC18*, whereas the second SRO loss maps to 1p21.3 and includes only two known coding genes, *PTBP2* and *DPYD*, and *miR-137*, a putative microRNA predicted (TargetScan; PicTar) to target the *MITF*, among others, and obviously warrants further analysis.

Table 2 Altered regions that co-exist more often than expected by chance ($P < 0.05$)

Cytogenetic location	Cytogenetic location	P-value
Gain of 1p12–q31.1	Gain of 1q31.3–qter	0.0000
Gain of 8q12.1–q23.1	Gain of 8q23.3–qter	0.0000
Loss of 8p23.3–p23.1	Gain of 8q12.1–q23.1	0.0017
Gain of 15q22.2–q26.3	Gain of chromosome 20	0.0047
Gain of chromosome 7	Loss of chromosome 10	0.0067
Gain of 1q31.3–qter	Loss of 6q12–qter	0.0155
Loss of 11q14.1–q25	Gain of chromosome 20	0.0155
Loss of chromosome 4	Gain of chromosome 20	0.0164
Loss of 8p23.3–p23.1	Loss of 22q12.3–qter	0.0171
Loss of chromosome 10	Gain of 17q21.31–qter	0.0234
Gain of 8q23.3–qter	Loss of 22q12.3–qter	0.0347

High frequency of copy number gains were found on 7q21.13–q31.1 and includes *CDK6*, encoding a p16INK4a antagonist, reported in increased gene copy numbers in ~35% of ultraviolet-induced murine melanomas (Kannan *et al.*, 2003). A second and more distal SRO gain maps to 7q32.1–q34 and includes *BRAF*, earlier found to be involved in complex alteration patterns (Daniotti *et al.*, 2004). *CCND1* amplification has been associated with the acral subtype of melanomas (Sauter *et al.*, 2002) and here, 11q13 amplification was found in only three cell lines corroborating suggestions that *CCND1* is not a general CMM oncogene. A gene that requires further analysis in this respect is *CDK3* on 17q25.1, found to have an increased gene copy number in 57% of the cell lines. In contrast to the well-characterized cyclin D/*cdk4/6*-mediated inactivation of retinoblastoma protein (pRB) at the G1/S transition, cyclin C/*cdk3* is implicated in promoting G0 cell-cycle exit through pRB phosphorylation (Ren and Rollins, 2004).

An interesting adjacent gene on 17q23.2 is *TBX2*, highly expressed in melanoma cells where it plays an important role in maintaining proliferation and suppression of senescence (Vance *et al.*, 2005), possibly by downregulation of p21CIP1 and *CDKN2A/p19ARF* (Jacobs *et al.*, 2000; Vance *et al.*, 2005). *TBX2* is one of the known targets for *MITF* in melanocytes, and a strong candidate melanoma oncogene (Carreira *et al.*, 2000). Here, we showed that *TBX2* has an increased gene copy number in 43% of the cell lines. Moreover, *MITF* at 3p13, was amplified in three cell lines and showed increased gene copy number in 36% of the cell lines, supporting a role in progressive and metastatic melanoma. Additionally, recurrent amplification was found on 1p12, the smallest amplicon including only *NOTCH2* (Figure 2e). Intriguingly, a recent study has shown that Notch2 protein is significantly up regulated in dysplastic nevi and melanomas but not in common melanocytic nevi (Massi *et al.*, 2006). Notch proteins are transmembrane receptors that are activated by specific ligands and increase signaling via the MAPK and PI3K pathways in melanoma cells (Liu *et al.*, 2006). Well-known oncogenes such as *MDM2*, *CCNE1* and *BRAF* were each found amplified in single samples. High-level amplification with unknown target genes were also

identified, for example, EST69 melanoma cells had two distinct and narrow peaks on 18q11.2, spanning 950 and 870 kbp, respectively. The first peak contained six known genes including a *laminin alpha 3* gene thought to be involved in cell adhesion, signal transduction and differentiation of keratinocytes (McLean *et al.*, 2003), and the second peak included only *ZNF521*. A complex and intriguing amplification pattern was found on chromosome 5p in FM72 cells, including a large number (>20) of narrow peaks, each with only a few or a single gene.

CDKN2A is the major melanoma susceptibility gene and also a major tumor suppressor gene in nonfamilial melanoma (Grafstrom *et al.*, 2005). Homozygous *CDKN2A* deletions were identified in 27/47 cell lines emphasizing their importance in melanoma cells and *in vitro* establishment. Although frequent in cultured cells, *PTEN* homozygous deletions or somatic mutations are less common in primary melanomas, suggesting that this is a late genetic event or that epigenetic mechanisms are responsible for *PTEN* silencing in primary tumors (Pollock *et al.*, 2002). Moreover, *PTEN* is likely not the only target gene on chromosome 10. Interestingly, one cell line harbored a homozygous deletion on 10p11.21 spanning a single gene (*PARD3*), encoding an evolutionarily conserved protein and key regulator of epithelial and neural cell polarity and migration (Macara, 2004). Another novel homozygous deletion at 4q34 encompasses no known genes and was found in three samples. Whether this deletion is of biological importance in melanoma development or merely a copy number polymorphism is unknown. Finally, a homozygous deletion on 11q14 included the *RAB38* gene, a homolog to a 9q21 melanoma susceptibility gene candidate (Jönsson *et al.*, 2005a), and previously characterized as a melanocyte differentiating antigen, but also abundantly expressed in melanoma tissue (Zippelius *et al.*, 2006).

CDKN2A was affected by homozygous deletion, mutation or methylation in the majority of cell lines. As expected, the single-cell line that harbored a *CDK4* mutation was wild type for *CDKN2A*, but did show high-level *CCNE1* amplification. In addition, we also confirmed that *BRAF* and *NRAS* mutations are mutually exclusive (Maldonado *et al.*, 2003). However, our data also suggest that as there is no selection for coupled *PTEN* and *NRAS* mutations, both *PTEN* and *BRAF* mutation commonly occur in the same cells, emphasizing that *BRAF* is downstream of *NRAS* and does not affect the PI3K/*PTEN* pathway (Tsao *et al.*, 2004). By searching for similar patterns of copy number changes, 11 concomitantly altered genomic pairs appeared (Table 2). The two top pairs included changes located on the same chromosome arm, possibly reflecting mechanistically related events. However, chromosome 7 gain was significantly correlated with chromosome 10 loss, functionally in accordance with coupled *BRAF* and *PTEN* mutation. Moreover, gain of chromosome 20 was correlated to gain of 15q22.2–q26.3, loss of 11q14.1–q25 and loss of chromosome 4. Another combination of interest was chromosome 10 loss and 17q21.31–qter gain, both regions including

potential genes such as *PTEN* and *CDK3/TBX2*, respectively.

These patterns suggest that mutations in key genes, such as *BRAF*, *NRAS*, *PTEN* or *TP53*, can direct pathogenesis and the genomic pathways leading to specific melanoma phenotypes. Accordingly, global gene expression analysis was recently used to identify a set of 80 genes that separated *BRAF*-mutated and wild-type cell lines (Pavey *et al.*, 2004). We used two-sided *t*-test to show that *BRAF* mutated cells have a high frequency (84%) of copy number gain on large regions of chromosome 7, which includes the *BRAF* gene on 7q34. A recent study found that both the mutant *BRAF* and the wild-type allele are targeted in copy number gains (Christensen and Guldberg, 2005). Chromosome 7 gain was less common in *NRAS*-mutated cells, the only aberration occurring at a significantly different frequency in *NRAS* mutant (40%) and wild-type cells (14%) was 3q13 gain. This indicates that *BRAF*-mutated cells are more homogenous in their genomic profiles than *NRAS*-mutated samples, corroborating the idea that *BRAF* mutation is an early genetic event. We further revealed that *PTEN*-mutated samples displayed a high frequency of 1p22.1–p21.1 loss, affecting a 10 Mb region and >50 genes, among them an elusive melanoma susceptibility gene (Gillanders *et al.*, 2003).

In summary, we observed a considerable variety in genomic aberrations reflecting the heterogeneous nature of CMM. Careful molecular characterization of well-defined melanoma cell lines discloses the major genetic events that determine pathogenesis. Further analysis on clinical tumor samples will decipher more complex and hierarchical patterns and their relation to clinical outcome.

Materials and methods

Cell lines and culture

FM melanoma cell lines were established as described previously (Guldberg *et al.*, 1997b). SK-MEL-3, SK-MEL-28, SK-MEL-19 and SK-MEL-31 cells were obtained from the American-type culture collection and EST cell lines from the ESTDAB Cell Bank (<http://www.ebi.ac.uk/ipd/estdab/>). All cells were cultured and maintained in RPMI 1640 medium with 10% fetal bovine serum. All were derived from CMM patients except EST128, which was derived from a primary ocular melanoma (Table 1).

DNA isolation and mutation analysis

Genomic DNA for arrayCGH and mutation analysis was isolated using the nucleospin tissue DNA extraction kit (Machery–Nagel, Easton, PA, USA) or the purescript DNA isolation kit (Gentra Systems, Minneapolis, MN, USA). *BRAF*, *NRAS*, *TP53*, *PTEN*, *CDKN2A*, *CTNNB1* and *CDK4* were screened using a combination of PCR and denaturing gradient gel electrophoresis (Guldberg *et al.*, 1997a, b; Christensen and Guldberg, 2005). Analysis of *CDKN2A* for deletions, mutations and promoter methylation was carried out as previously described (Gronbaek *et al.*, 2000).

ArrayCGH

Microarrays were produced from the 32K BAC clone library (CHORI BACPAC Resources, <http://bacpac.chori.org/genomicRearrays.php>) at the SWEGENE DNA Micro-

array Resource Center. Mapping data for each BAC clone was based on build hg17 (UCSC May 2004). DOP-PCR products were obtained from BAC DNA template and purified using filter-based 96-wells plates (PALL, East Hills, NY, USA), dried and resuspended in 50% dimethyl sulfoxide to a concentration of 500–1000 ng/ μ l. Arrays were printed on UltraGAPS slides (Corning, Corning, NY, USA) using a MicroGrid II spotter (Biorobotics, Cambridge, UK) (Jönsson *et al.*, 2005a). For all samples, 2 μ g of genomic DNA was labeled using a random labeling kit (Invitrogen Life Technologies, Carlsbad, CA, USA) (Jönsson *et al.*, 2005b). Test DNA and male commercial reference DNA was differentially labeled, pooled, mixed with human COT-1 DNA, dried and resuspended in a formamide-based buffer. The hybridization reactions were applied to arrays, which were incubated under cover slips for 48–72 h at 37°C. Slides were washed (Snijders *et al.*, 2001) and scanned using an Agilent Microarray scanner (Agilent Technologies, Santa Clara, CA, USA). Identification of individual spots on scanned arrays was performed with Gene Pix Pro 4.0 (Axon Instruments, Weatherford, TX, USA), and the quantified data matrix was loaded into BioArray Software Environment (BASE) (Saal *et al.*, 2002). Background-correction of Cy3 and Cy5 intensities was calculated using the median-feature and median-local background intensities. Within arrays, intensity ratios for individual probes were calculated as background-corrected intensity of sample divided by background-corrected intensity of reference sample. A signal-to-noise filter of ≥ 5 for the sample and reference channels was applied, and spots that failed to pass these criteria were excluded. The filtered data was, for each array separately, centralized to a median ratio of unity excluding X and Y chromosome clones. All filtering, normalization and analysis were performed in BASE. Subsequently a moving average of 150 kbp was applied and a BASE implementation of CGH Plotter was used to determine deletion/amplicon boundaries (Autio *et al.*, 2003). The noise constant was set to 15 and the amplification/deletion limits were set to ± 0.2 . The noise constant is used to modulate the amount of segmental breakpoints on each chromosome. A high-noise constant corresponds to a large number of breakpoints per chromosome. CGH Plotter returned a sample data set transformed to a ternary scale (–1, 0 and 1) corresponding to (loss, normal and gain) for 27834 BACs as described (Jönsson *et al.*, 2005b). Amplification was defined as gains exceeding a \log_2 (ratio) > 1.5 and homozygous deletions were considered when a \log_2 (ratio) ≤ -2 was observed.

Statistical analysis

Identification of regions associated with specific-mutated genes was performed using a standard two-sided two-sample *t*-test for individual BAC clones. The analysis of pair-wise genomic regions was performed as follows. Genomic regions, defined as two or more sequential gained or lost clones, altered in at least 40% of the cell lines were identified and recoded as binary variables (1 for gain/loss and 0 for no alteration). A 10% in the frequency variation was accepted inside a region, and consequently the end of an amplified region was determined by two or more consecutive clones with a frequency inferior to 36%. Associations between copy number changes, that is, analysis of whether certain alterations occurred more (or less) often than expected under the null hypothesis of no association, were evaluated using a permutation test. For each pair of two alterations, the observed number of co-events was compared to the null distribution constructed by simulating 10 000 replicates conditional on the observed marginal totals. All associations with $P < 0.05$ were listed in Table 2. It should

be noted that only those with $P < 0.0001$ were considered significant after Bonferroni correction for multiple comparisons, most probably a too conservative correction. The same permutation-based association analysis was used when searching for excess co-occurrence of gene-specific point mutations. Data from EST128 were not included.

Acknowledgements

This work was supported by grants from the Swedish Cancer Society, the Swedish Research Council, the Mrs Berta

Kamprad Foundation, the Gunnar Nilsson Cancer Foundation, the Franke & Margareta Bergqvist Foundation, the American Cancer Society, the Lund University Hospital Foundations, the King Gustav Vs Jubilee Foundation, the Ingabritt and Arne Lundberg Foundation, the Swedish Foundation for Strategic Research, the Marianne and Marcus Wallenberg Foundation and by the Knut and Alice Wallenberg Foundation via the SWEGENE program. The support from Pieter de Jong and Kazutoyo Osoegawa, BACPAC Resource Center at CHORI, is acknowledged.

References

- Autio R, Hautaniemi S, Kauraniemi P, Yli-Harja O, Astola J, Wolf M *et al.* (2003). CGH-Plotter: MATLAB toolbox for CGH-data analysis. *Bioinformatics* **19**: 1714–1715.
- Bittner M, Meltzer P, Chen Y, Jiang Y, Seftor E, Hendrix M *et al.* (2000). Molecular classification of cutaneous malignant melanoma by gene expression profiling. *Nature* **406**: 536–540.
- Cachia AR, Indsto JO, McLaren KM, Mann GJ, Arends MJ. (2000). CDKN 2A mutation and deletion status in thin and thick primary melanoma. *Clin Cancer Res* **6**: 3511–3515.
- Carreira S, Liu B, Goding CR. (2000). The gene encoding the T-box factor Tbx2 is a target for the microphthalmia-associated transcription factor in melanocytes. *J Biol Chem* **275**: 21920–21927.
- Christensen C, Guldberg P. (2005). Growth factors rescue cutaneous melanoma cells from apoptosis induced by knockdown of mutated (V 600 E) B-RAF. *Oncogene* **24**: 6292–6302.
- Curtin JA, Fridlyand J, Kageshita T, Patel HN, Busam KJ, Kutzner H *et al.* (2005). Distinct sets of genetic alterations in melanoma. *N Engl J Med* **353**: 2135–2147.
- Daniotti M, Oggionni M, Ranzani T, Vallacchi V, Campi V, Di Stasi D *et al.* (2004). BRAF alterations are associated with complex mutational profiles in malignant melanoma. *Oncogene* **23**: 5968–5977.
- Gillanders E, Juo SH, Holland EA, Jones M, Nancarrow D, Freas-Lutz D *et al.* (2003). Localization of a novel melanoma susceptibility locus to 1p22. *Am J Hum Genet* **73**: 301–313.
- Grafstrom E, Egyhazi S, Ringborg U, Hansson J, Platz A. (2005). Biallelic deletions in INK4 in cutaneous melanoma are common and associated with decreased survival. *Clin Cancer Res* **11**: 2991–2997.
- Gronbaek K, de Nully Brown P, Moller MB, Nedergaard T, Ralfkiaer E, Holler P *et al.* (2000). Concurrent disruption of p16INK4a and the ARF-p53 pathway predicts poor prognosis in aggressive non-Hodgkin's lymphoma. *Leukemia* **14**: 1727–1735.
- Guldberg P, Nedergaard T, Nielsen HJ, Olsen AC, Ahrenkiel V, Zeuthen J. (1997a). Single-step DGGE-based mutation scanning of the p53 gene: application to genetic diagnosis of colorectal cancer. *Hum Mutat* **9**: 348–355.
- Guldberg P, thor Straten P, Birck A, Ahrenkiel V, Kirkin AF, Zeuthen J. (1997b). Disruption of the MMAC1/PTEN gene by deletion or mutation is a frequent event in malignant melanoma. *Cancer Res* **57**: 3660–3663.
- Haqq C, Nosrati M, Sudilovsky D, Crothers J, Khodabakhsh D, Pulliam BL *et al.* (2005). The gene expression signatures of melanoma progression. *Proc Natl Acad Sci USA* **102**: 6092–6097.
- Hayward NK. (2003). Genetics of melanoma predisposition. *Oncogene* **22**: 3053–3062.
- Jacobs JJ, Keblusek P, Robanus-Maandag E, Kristel P, Lingbeek M, Nederlof PM *et al.* (2000). Senescence bypass screen identifies TBX2, which represses Cdkn2a (p19(ARF)) and is amplified in a subset of human breast cancers. *Nat Genet* **26**: 291–299.
- Jönsson G, Bendahl PO, Sandberg T, Kurbasic A, Staaf J, Sunde L *et al.* (2005a). Mapping of a novel ocular and cutaneous malignant melanoma susceptibility locus to chromosome 9q21.32. *J Natl Cancer Inst* **97**: 1377–1382.
- Jönsson G, Naylor TL, Vallon-Christersson J, Staaf J, Huang J, Ward MR *et al.* (2005b). Distinct genomic profiles in hereditary breast tumors identified by array-based comparative genomic hybridization. *Cancer Res* **65**: 7612–7621.
- Kannan K, Sharpless NE, Xu J, O'Hagan RC, Bosenberg M, Chin L. (2003). Components of the Rb pathway are critical targets of UV mutagenesis in a murine melanoma model. *Proc Natl Acad Sci USA* **100**: 1221–1225.
- Liu ZJ, Xiao M, Balint K, Smalley KS, Brafford P, Qiu R *et al.* (2006). Notch1 signaling promotes primary melanoma progression by activating mitogen-activated protein kinase/phosphatidylinositol 3-kinase-Akt pathways and up-regulating N-cadherin expression. *Cancer Res* **66**: 4182–4190.
- Macara IG. (2004). Parsing the polarity code. *Nat Rev Mol Cell Biol* **5**: 220–231.
- Maldonado JL, Fridlyand J, Patel H, Jain AN, Busam K, Kageshita T *et al.* (2003). Determinants of BRAF mutations in primary melanomas. *J Natl Cancer Inst* **95**: 1878–1890.
- Massi D, Tarantini F, Franchi A, Paglierani M, Di Serio C, Pellerito S *et al.* (2006). Evidence for differential expression of Notch receptors and their ligands in melanocytic nevi and cutaneous malignant melanoma. *Modern Pathol* **19**: 616.
- McLean WH, Irvine AD, Hamill KJ, Whittock NV, Coleman-Campbell CM, Mellerio JE *et al.* (2003). An unusual N-terminal deletion of the laminin alpha3a isoform leads to the chronic granulation tissue disorder laryngo-onycho-cutaneous syndrome. *Hum Mol Genet* **12**: 2395–2409.
- Omholt K, Platz A, Kanter L, Ringborg U, Hansson J. (2003). NRAS and BRAF mutations arise early during melanoma pathogenesis and are preserved throughout tumor progression. *Clin Cancer Res* **9**: 6483–6488.
- Pavey S, Johansson P, Packer L, Taylor J, Stark M, Pollock PM *et al.* (2004). Microarray expression profiling in melanoma reveals a BRAF mutation signature. *Oncogene* **23**: 4060–4067.
- Pollock PM, Harper UL, Hansen KS, Yudt LM, Stark M, Robbins CM *et al.* (2003). High frequency of BRAF mutations in nevi. *Nat Genet* **33**: 19–20.

- Pollock PM, Walker GJ, Glendening JM, Que Noy T, Bloch NC, Fountain JW *et al.* (2002). PTEN inactivation is rare in melanoma tumours but occurs frequently in melanoma cell lines. *Melanoma Res* **12**: 565–575.
- Ren S, Rollins BJ. (2004). Cyclin C/cdk3 promotes Rb-dependent G0 exit. *Cell* **117**: 239–251.
- Saal LH, Troein C, Vallon-Christersson J, Gruvberger S, Borg A, Peterson C. (2002). BioArray Software Environment (BASE): a platform for comprehensive management and analysis of microarray data. *Genome Biol* **3**: software0003.
- Sauter ER, Yeo UC, von Stemm A, Zhu W, Litwin S, Tichansky DS *et al.* (2002). Cyclin D1 is a candidate oncogene in cutaneous melanoma. *Cancer Res* **62**: 3200–3206.
- Snijders AM, Nowak N, Segreaves R, Blackwood S, Brown N, Conroy J *et al.* (2001). Assembly of microarrays for genome-wide measurement of DNA copy number. *Nat Genet* **29**: 263–264.
- Takata M, Goto Y, Ichii N, Yamaura M, Murata H, Koga H *et al.* (2005). Constitutive activation of the mitogen-activated protein kinase signaling pathway in acral melanomas. *J Invest Dermatol* **125**: 318–322.
- Tanami H, Imoto I, Hirasawa A, Yuki Y, Sonoda I, Inoue J *et al.* (2004). Involvement of overexpressed wild-type BRAF in the growth of malignant melanoma cell lines. *Oncogene* **23**: 8796–8804.
- Tsao H, Goel V, Wu H, Yang G, Haluska FG. (2004). Genetic interaction between NRAS and BRAF mutations and PTEN/MMAC1 inactivation in melanoma. *J Invest Dermatol* **122**: 337–341.
- Tucker MA, Goldstein AM. (2003). Melanoma etiology: where are we? *Oncogene* **22**: 3042–3052.
- Walker GJ, Indsto JO, Sood R, Faruque MU, Hu P, Pollock PM *et al.* (2004). Deletion mapping suggests that the 1p22 melanoma susceptibility gene is a tumor suppressor localized to a 9-Mb interval. *Genes Chromosomes Cancer* **41**: 56–64.
- Vance KW, Carreira S, Brosch G, Goding CR. (2005). Tbx2 is overexpressed and plays an important role in maintaining proliferation and suppression of senescence in melanomas. *Cancer Res* **65**: 2260–2268.
- Zippelius A, Gati A, Bartnick T, Walton S, Odermatt B, Jaeger E *et al.* (2006). Melanocyte differentiation antigen RAB38/NY-MEL-1 induces frequent antibody responses exclusively in melanoma patients. *Cancer Immunol Immunother* Epub ahead of print.